INFILTRATION CAPACITY DERIVATIVES AND SOIL MOISTURE EQUATION MODEL VALIDATION

Martheana Kencanawati[1], Data Iranata[2], Mahendra Andiek Maulana[2], A. A. Ngurah Satria Damarnegara[2]

[1] Department Civil Engineering, University of Balikpapan, Balikpapan, Indonesia
[2] Department Civil Engineering, Institut Teknologi Sepuluh Nopember, Surabaya, Indonesia

E-mail: martheana@uniba-bpn.ac.id

Received: May 11, 2025	**Accepted:** July 27, 2025	**Published:** July 27, 2025
DOI: 10.12962/j27745449.v5i3.4183	**Issue:** Volume 5 Number 3 2024	**E-ISSN:** 2774-5449

ABSTRACT

Infiltration is an essential parameter in runoff, although its simulation remains challenging due to soil heterogeneity and complex structures. As soil moisture increases, infiltration capacity decreases nonlinearly, stabilizing when saturation is reached. Therefore, this study aimed to improve and validate the Horton Equation using field observations to determine infiltration capacity in watersheds. Overland flow observations were used to assess simulation accuracy from the previous studies, the sensitivity curve number was obtained at a range of 49–57. The results showed that high precipitation saturated initial losses and infiltration capacity, producing a greater runoff coefficient. The sensitivity curve numbers were obtained differently between Pandantoyo sub-basin (CN 49–53) and Ngadirejo sub-basin (CN 53–55). From modification runoff coefficient values (dimensionless,) for an ungauged catchment, it could be obtained function of f ($R_{24,}$ S_m), LU. Soil moisture value between Pandantoyo and Ngadirejo sub-basin was 3,562. It was also discovered that C was Q from AWLR observation and time of concentration, which influenced water discharge. A longer Tc led to lower discharge without increasing water levels. Furthermore, SCS Direct runoff method had minimal impact on runoff coefficients.

Keyword: Soil moisture, soil water, infiltration, curve number, Horton equation

Introduction

Infiltration is an essential parameter in runoff, although its simulation remains challenging due to soil heterogeneity and complex structures [1]. Infiltration capacity decreases nonlinearly with increased soil moisture, stabilizing when saturation is reached. Therefore, the improved Horton Equation and field observations are applied to determine infiltration capacity, validated by overland flow observations [1,2]. Previous studies have shown that soil types C and D, with lower infiltration rates, generate significant runoff, contributing to a larger runoff coefficient [1].

In this context, simulating soil water infiltration is essential in hydrology but challenging due to heterogeneous soils and complex structures [3,4,5]. Each soil surface has an absorption capacity whose ability varies from soil condition and the surface cover layer [5][6]. Infiltration capacity decreases nonlinearly as soil moisture increases, stabilizing when soil is saturated [5]. To address the challenge, this study used primary data collection and numerical methods to explore the relationship between infiltration capacity and soil moisture [6]. In addition to classifying infiltration, infiltration rates were compared across various soil types to measure macropore flow [6].

Rainfall infiltration is generally influenced by soil type, porosity, texture, vegetation cover, land management, and preferential flow due to roots, cracks, and soil fauna. In natural systems, the macropores in soil can rapidly store significant quantities of infiltrated water as well as pollutants, particularly during periods of intense rainfall, thereby affecting shallow and steep water bodies [6,7]. To capture the dynamics of infiltration, the power function is fit to soil moisture-time curve data and adopted to describe the nonlinear relationship between infiltration capacity and soil moisture [7,8,9]. Infiltration process at the ground level of the watershed has a substantial impact on both the timing as well as the magnitude of high and low-flow events [10,11]. Therefore, this study aimed to model nonlinear infiltration behavior using a power equation that best represented soil moisture dynamics observed in the field.

Methodology

Infiltration measurements can be used for a variety of study purposes, including to estimate relevant soil hydraulic parameters by fitting infiltration data to inverted models [12,13]. As soil moisture increases, infiltration capacity decreases nonlinearly, stabilizing when saturation is reached. Therefore, this study aimed to improve and validate the Horton Equation using field observations to determine infiltration capacity in watersheds. Overland flow observations were used to assess the accuracy of the simulation [14]. Furthermore, fieldwork and HEC HMS model simulations were combined to determine runoff coefficients.

Result and Discussion

The decrease in the value of infiltration capacity reduces with time until it is close to a constant value of 40 minutes, as shown in Figure 1.

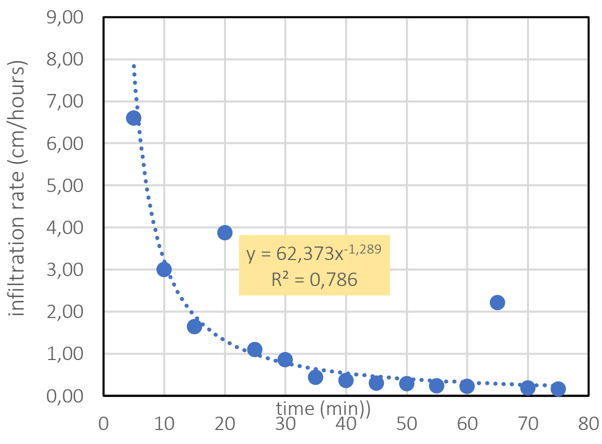

Figure 1. Infiltration rate of sandy loam [15]

This decrease in infiltration capacity is influenced by factors that occur at soil surface compared to the processes that flow in soil [16]. When precipitation increases, the initial losses and infiltration capacity will meet (saturate). The runoff also increases, thereby causing a higher runoff coefficient. In previous studies, it was stated that a small infiltration rate with soil types C and D would produce a large runoff, leading to a greater runoff coefficient [1].

In this study, the results were obtained that infiltration rate was classified as soil type A and produced small runoff with lower coefficient. The value of the flow coefficient at 0.4 for rice fields is greater than the results produced from field experiments. From a previous study [14], excessive rainfall increases runoff coefficients due to higher intensity leading to expanded surface runoff. The runoff coefficient is calculated using the formula method by dividing the runoff volume by rainfall volume [14]. For instance, when rainfall over 24 hours (R_{24}) is 48 mm, this calculation can be conducted over a watershed area of 91,526 km^2 [15].

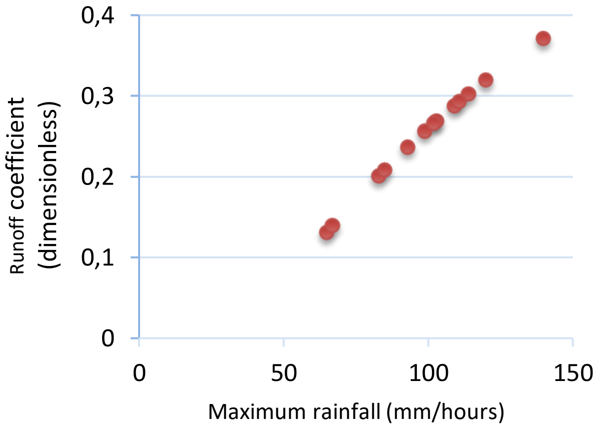

Figure 2. Correlation between runoff coefficient and maximum rainfall intensity from 2010 to 2022[15].

The relationship described in Figure 2 indicates that higher maximum rainfall conditions will lead to an increase in the flow coefficient. This proves that high rainfall intensity results in greater surface water runoff. Lanang River basin, which is approximately 40 km in length, shows a lower surface runoff rate compared to a widened basin with the same overall area.

To calculate rainfall volume, multiply R_{24} by the area:

Rainfall volume

$= R_{24} x\ A$

$= 48\ mm\ x\ 91{,}526\ km^2$

$= 0.000048\ km\ x\ 91.526\ km^3$

$= 0.00439\ km^3$

$= 4.39\ m^3$

Rain volume of 4.39 m^3 will be used to estimate direct runoff.

Table 1 shows the identified parameter k' in the Improved Horton Equation to be 0.5 for value $\boldsymbol{f_c f_0}$.

Table 1. Calibrated Parameters for Original and Improved Horton Equations [15]

Parameter	Original Horton Equation	Original Horton Equation
f_0	100-500	100-500
f_c	15-100	15-100
k	0 - 30	none
k'	none	0,5 - 5

Table 1 shows improved Horton Equation, with the following assumption k' is 0.5, P is 0 mm/hour, ET is 0, and e equals 2.781. Rainfall is represented by P, and evapotranspiration by ET. During runoff events, ET simulation can be omitted as it occurs instantaneously [15].

$$R(\theta) = P - ET - f$$

$$R(\theta) = P - ET - \ f_c - (f_0 - f_c)\boldsymbol{e}^{-\boldsymbol{k}(\frac{\boldsymbol{\theta}-\boldsymbol{\theta_0}}{\theta_0-\theta_c})}$$

$$= 0\text{-}0\text{-}90\text{-}(240\text{-}90).\ \boldsymbol{e}^{-\mathbf{0,5}(\frac{\boldsymbol{\theta}-\boldsymbol{\theta_0}}{\theta_0-\theta_c})}$$

$$= \text{-}90\text{-}150.\ \boldsymbol{e}^{-\mathbf{0,5}(\frac{\boldsymbol{\theta}-\boldsymbol{\theta_0}}{\theta_0-\theta_c})}$$

assume $\left(\frac{\boldsymbol{\theta}-\boldsymbol{\theta_0}}{\theta_0-\theta_c}\right) = \boldsymbol{Sm}$

hence: $\boldsymbol{e}^{-\mathbf{0,5}\boldsymbol{Sm}} = \frac{R(\theta)+90}{-150}$

Derrivative function $f(x_1) = \boldsymbol{e}^{-\mathbf{0,5}\boldsymbol{Sm}}$

And $f(x_2) = \frac{R(\theta)+27}{-39}$

$$f(x_1) = f(x_2)$$

$$f'^{(x_1)} = f'^{(x_2)}$$

$$-0{,}5Sm - 1.e = 1$$

Assumes: e = 2.781, hence

$$-0{,}5Sm - 1.2{,}781 = 1$$

$$-0{,}5Sm = 1 - 2{,}781$$

$$Sm = \frac{1 - 2{,}781}{-0{,}5} = 3{,}562$$

Soil moisture between Pandantoyo and Ngadirejo sub-basin is 3,562. Furthermore, automatic water level recorder observations and the time of concentration ascertain that C is Q. Longer concentration time reduces water discharge without increasing levels. SCS Direct runoff method minimally impacts runoff coefficients.

Sensitivity analysis of CN in the model ranges from 35 to 99. Modeling results indicate that CN Pandantoyo values range between 49 and 58, while N.C. values vary between 50 and 55[14]. To calculate surface runoff in a catchment area, this study used SCS NRCS runoff method based on characteristics obtained from maps or field observations [14,15]. The results showed that the area's soil type A had a low infiltration rate and runoff coefficient [14].

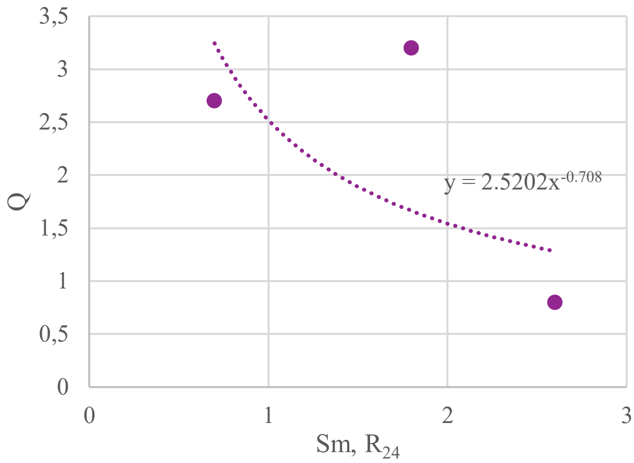

Figure. 1 Impact of Q from AWLR observation on C and daily soil moisture precipitation [15]

Table 2. Q value of HMS HMS to C in Pandantoyo Sub Watershed

Sub DAS	$Q_{HEC\ HMS}$ (m^3/s)	C
Ngadirejo	0.26	0.36
	0.32	0.45
	0.39	0.55
Pandantoyo	0.29	0.01
	0.29	0.01
	0.28	0.01
	0.26	0.01

From Table 2, it can be described that the typical flow coefficient value used, with a range of 0.4 for rice fields, is higher than the runoff coefficient obtained from field experiments. This shows that Pandantoyo Village's rice field has higher infiltration rates than Ngadirejo Village's garden land and bushes [15]. The disparity in results can be attributed to land cover, which affects watershed characteristics. Pandantoyo features slope terrains used for sugarcane plantations, while Ngadirejo has experienced substantial land conversion [15]. The elongated and narrow configuration of a watershed minimizes surface runoff compared to broader watersheds [15]. Generally, direct runoff is calculated with the R_{24} method, and average rainfall using Thiessen polygon method. The steps to find C observed are with Rain Volume data and Hydrograph Unit data [13].

$$\varphi \text{ index} = \frac{P-R}{T}$$

When P represents rainfall exceeding the index, R is the total runoff, and T is the duration of effective rainfall. An index is defined as the saturated infiltration rate, where rainfall volume equals runoff volume [15,18,19]. C observed is assigned a value of 0.4 because it falls in the category of rice fields, as referenced in [15].

$$C = \frac{daily\ precipitation\ volume}{R_{24}.A}$$

In this equation, C observed can be defined as φ index and with Area A = 91,526 km2

Table 3. Daily Rainfall Volume and Discharge

Number of data	Date	H	Q AWLR	Q Average	R_{24}
538	06/02/22	0.62	0.74	0.68	24
658	06/07/22	0.66	0.80	0.75	48
730	06/10/22	0.52	0.57	0.69	63
850	06/15/22	0.65	0.79	0.97	29
898	06/17/22	0.76	0.98	0.96	44
970	06/20/22	0.79	1.05	0.89	34
1090	06/25/22	0.63	0.74	0.72	27

The key factors affecting runoff include the percentage of watertight area and the curve number (CN) [15]. A higher curve number indicates increased runoff, in theoretical constraints [17,18]. An increase in precipitation saturates initial losses and infiltration capacity, which produces a higher runoff coefficient [19,20,21].

Conclusion

In conclusion, this study showed significant adjustments to runoff coefficient values (dimensionless). For an ungauged catchment, it could be obtained as a function of f (R_{24}, Sm), LU. Soil moisture value between Pandantoyo and Ngadirejo sub-basin was 3,562. This showed that C was Q from AWLR observation, and the time of concentration influenced water discharge. A longer Tc produced lower discharge without raising water levels. SCS Direct Runoff method had minimal impact on runoff coefficient.

Acknowledgements

The authors acknowledge the support from Universitas Balikpapan Yapenti DWK East Kalimantan, the Kaltim Tuntas Scholarship, and PT Bayan Resources TBK during the study. The authors also appreciate the data provided by PU SDA East Java and the proofreading assistance from Native-Proofreading.com.

References

[1] M. Yang, Y. Zhang, and X. Pan, Improving the Horton infiltration equation by considering soil moisture variation, *Journal of Hydrology*, **586** (2020) 124864. DOI: 10.1016/j.jhydrol.2020.124864.

[2] S. di Prima, R. D. Stewart, M. R. Abou Najm, D. Yilmaz, A. Comegna, and L. Lassabatere, Modeling water infiltration into soil under fractional wettability conditions, *Journal of Hydrology*, **647** (2025) 132309. DOI: 10.1016/j.jhydrol.2024.132309.

[3] H. Feng, X. Xing, J. Xing, J. Du, and D. Li, Performance and modeling of infiltration flow in cracked saline soils, *Journal of Hydrology*, **656** (2025) 133054. DOI: 10.1016/j.jhydrol.2025.133054.

[4] Y. Li *et al.*, Multi-model analysis of historical runoff changes in the Lancang-Mekong River Basin – Characteristics and uncertainties, *Journal of Hydrology*, **619** (2023) 129297. DOI: 10.1016/j.jhydrol.2023.129297.

[5] S. di Prima, R. D. Stewart, M. R. Abou Najm, D. Yilmaz, A. Comegna, and L. Lassabatere, Modeling water infiltration into soil under fractional wettability conditions, *Journal of Hydrology*, **647** (2025) 132309. DOI: 10.1016/j.jhydrol.2024.132309.

[6] C. Basset, M. Abou Najm, T. Ghezzehei, X. Hao, and A. Daccache, How does soil structure affect water infiltration? A meta-data systematic review, *Soil and Tillage Research*, **226** (2023) 105577. DOI: 10.1016/j.still.2022.105577.

[7] S. Wu, T. F. M. Chui, and L. Chen, Modeling slope rainfall-infiltration-runoff process with shallow water table during complex rainfall patterns, *Journal of Hydrology*, **599** (2021) 126458. DOI: 10.1016/j.jhydrol.2021.126458.

[8] C. B. Bergeson, K. L. Martin, B. Doll, and B. B. Cutts, Soil infiltration rates are underestimated by models in an urban watershed in central North Carolina, USA, *Journal of Environmental Management*, **313** (2022) 115004. DOI: 10.1016/j.jenvman.2022.115004.

[9] J. Song *et al.*, Comparison between different infiltration models to describe the infiltration of permeable brick pavement system via a laboratory-scale experiment, *Water Science and Technology*, **84**(9) (2021) 2214–2227.

[10] K. G. Hopkins, A. S. Bhaskar, S. A. Woznicki, and R. M. Fanelli, Changes in event-based streamflow magnitude and timing after suburban development with infiltration-based stormwater management, *Hydrological Processes*, **34**(2) (2020) 387–403.

[11] H. McMillan, Linking hydrologic signatures to hydrologic processes: A review, *Hydrological Processes*, **34**(6) (2020) 1393–1409.

[12] P. J. Edwards, K. W. J. Williard, and J. E. Schoonover, Fundamentals of watershed hydrology, *Journal of Contemporary Water Research & Education*, **154**(1) (2015) 3–20.

[13] J. W. Hopmans, Infiltration and unsaturated zone, in: P. B. Wilderer (Ed.), *Treatise on Water Science*, Elsevier, 2011, pp. 103–114. DOI: 10.1016/B978-0-444-53199-5.00031-2.

[14] M. Kencanawati and M. A. Maulana, An advanced empirical NRCS-CN model estimation for ungauged catchment insufficient data, *International Journal on Advanced Science, Engineering and Information Technology*, **14**(2) (2024). DOI: 10.18517/ijaseit.14.2.19810.

M. Kencanawati, A modified rational method for determining runoff coefficient based on time series data in Pandantoyo and Ngadirejo Subbasin, Doctoral dissertation, Institut Teknologi Sepuluh Nopember, 2024. Available: https://repository.its.ac.id/113621/

[15] L. D. Susanawati, B. Rahadi, and Y. Tauhid, Determining the infiltration rate using double ring infiltrometer measurements and Horton model calculations in a tangerine (*Citrus reticulata*) orchard in Selorejo Village, Malang Regency, *Jurnal Sumberdaya Alam dan Lingkungan*, **5**(2) (2018). DOI: 10.21776/ub.jsal.2018.005.02.4.

[16] K. Mishra, H. L. Tiwari, and M. S. Hora, Assessment of rainfall-runoff relation in watershed using SCS curve number method, in: M. Pandey, N. V. Umamahesh, J. Das, and J. H. Pu (Eds.), *Hydrology and Hydrologic Modelling*, Springer Nature, Singapore, 2025, pp. 163–172.

[17] Q. Sun and J. Liu, The impact of rainfall value on the accuracy of the SCS-CN model: Selection of model parameters, *AQUA - Water Infrastructure, Ecosystems and Society*, **74**(1) (2024) 142–158. DOI: 10.2166/aqua.2024.288.

[18] X. Ren, N. Hong, L. Li, J. Kang, and J. Li, Effect of infiltration rate changes in urban soils on stormwater runoff process, *Geoderma*, **363** (2020) 114158.

[19] X. Wang *et al.*, Response of soil water in deep dry soil layers to monthly precipitation, plant species, and surface mulch in a semi-arid hilly loess region of China, *Agricultural Water Management*, **291** (2024) 108612. DOI: 10.1139/cgj-2023-0223.

[20] C. Langhans *et al.*, Experimental rainfall-runoff data: Reconsidering the concept of infiltration capacity, *Journal of Hydrology*, **399**(3–4) (2011) 255–262.